RL-TR-95-4
Final Technical Report
January 1995

MATSurv MULTISENSOR AIR TRAFFIC SURVEILLANCE

University of Connecticut

Murali Yeddanapudi, Yaakov Bar-Shalom, Krishna R. Pattipati,
T. Kirubarajan, and Somnath Deb

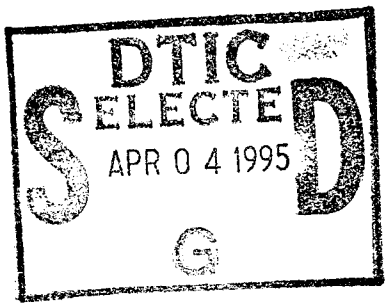

APPROVED FOR PUBLIC RELEASE; DISTRIBUTION UNLIMITED.

Rome Laboratory
Air Force Materiel Command
Griffiss Air Force Base, New York

This report has been reviewed by the Rome Laboratory Public Affairs Office (PA) and is releasable to the National Technical Information Service (NTIS). At NTIS it will be releasable to the general public, including foreign nations.

RL-TR-95-4 has been reviewed and is approved for publication.

APPROVED: Richard R. Gassner

RICHARD R. GASSNER
Project Engineer

FOR THE COMMANDER: Donald W. Hanson

DONALD W. HANSON
Director of Surveillance & Photonics

If your address has changed or if you wish to be removed from the Rome Laboratory mailing list, or if the addressee is no longer employed by your organization, please notify RL (OCTM) Griffiss AFB NY 13441. This will assist us in maintaining a current mailing list.

Do not return copies of this report unless contractual obligations or notices on a specific document require that it be returned.

REPORT DOCUMENTATION PAGE

Form Approved
OMB No. 0704-0188

1. AGENCY USE ONLY (Leave Blank)	2. REPORT DATE	3. REPORT TYPE AND DATES COVERED
	January 1995	Final May 93 - Aug 94

4. TITLE AND SUBTITLE

MATSurv MULTISENSOR AIR TRAFFIC SURVEILLANCE

5. FUNDING NUMBERS

C - F30602-93-C-0090
PE - 61102F
PR - 2304
TA - E8
WU - P7

6. AUTHOR(S)

Murali Yeddanapudi, Yaakov Bar-Shalom,
Krishna R. Pattipati, T. Kirubarajan, and Somnath Deb

7. PERFORMING ORGANIZATION NAME(S) AND ADDRESS(ES)

University of Connecticut
Dept of Electrical & Systems Engineering
Storrs CT 06269-3157

8. PERFORMING ORGANIZATION REPORT NUMBER

N/A

9. SPONSORING/MONITORING AGENCY NAME(S) AND ADDRESS(ES)

Rome Laboratory (OCTM)
26 Electronic Pky
Griffiss AFB NY 13441-4514

10. SPONSORING/MONITORING AGENCY REPORT NUMBER

RL-TR-95-4

11. SUPPLEMENTARY NOTES

Rome Laboratory Project Engineer: Richard R. Gassner/OCTM/(315) 330-3574

12a. DISTRIBUTION/AVAILABILITY STATEMENT

Approved for public release; distribution unlimited.

12b. DISTRIBUTION CODE

13. ABSTRACT (Maximum 200 words)

In this report, the results of the work on multisensor air traffic surveillance and a description of MATSurv, a software tool for tracking multiple targets using measurements from asynchronous sensors, are presented. The work addresses the issues of modeling the target motion, estimating target states, and determining a consistent set of measurement-target associations. The specific objectives of this work are to formulate and solve the data association problem for actual tracking scenarios with multiple, multimodality sensor subsystems. Two phases of the work are described, namely, the tuning phase whereby the measurements are associated with the appropriate targets using the known target IDs to tune and validate the tracking filter, and the assignment phase whereby the association is carried out using a two-dimensional assignment algorithm developed at UConn. Also, the performance of the tracking and assignment algorithms using three representative sets of measurements is illustrated.

14. SUBJECT TERMS	15. NUMBER OF PAGES
Multisensor multitarget data fusion, Tracking, Surveillance	44
	16. PRICE CODE

17. SECURITY CLASSIFICATION OF REPORT	18. SECURITY CLASSIFICATION OF THIS PAGE	19. SECURITY CLASSIFICATION OF ABSTRACT	20. LIMITATION OF ABSTRACT
UNCLASSIFIED	UNCLASSIFIED	UNCLASSIFIED	UL

1 Introduction

A surveillance and tracking system consists of a network of geographically and functionally distributed sensors (e.g., L-band, S-band, C-band, infrared). The objective of such a system is to detect an *unknown* number of targets in its field of view and estimate the states (target position, velocity, acceleration, etc.) using sensor measurements contaminated by noise. This must be accomplished in the presence of spurious observations (created by background noise and clutter) and occasional missed detections by sensors.

The tracking process, as generally practiced today, consists of four interrelated functions:

1. Selection of the state variable models used to represent the target motion and sensor measurements, including models of clutter and measurements uncertainties,

2. Evaluation of an index of desirability for each candidate measurement-target association,

3. Determination of a consistent set of measurement-target associations, and

4. Estimation of target states.

Association is the decision process of *linking* measurements of a common origin (i.e., a target or false alarms) such that each measurement is associated with only one origin. A set of linked measurements can then be *statistically filtered* to *estimate* the states of targets. With the ever increasing demand for higher performance in surveillance and tracking systems, it behooves us to consider novel methods of associating data from multiple, multi-modality sensor subsystems, and to estimate target states.

As part of the research effort for Rome Laboratories, the University of Connecticut (UConn) is transitioning the data association and estimation algorithms, developed as part of AFOSR funded research, to actual tracking problems of interest to the Air Force. The specific objectives of this work are:

- Develop the maximum likelihood formulation of the data association problem for actual tracking scenarios with multiple, multi-modality sensor subsystems;
- Develop algorithms for solving the data association problem; and
- Demonstrate the effectiveness of models/algorithms on *track initiation problem* using the RL surveillance testbed.

We approached the data association and track initiation problem in two phases:

1. **Phase 1:** All measurements are correctly associated with the appropriate targets based on target ID (from the beacon returns) to validate the filter design and fine tune the tracking filter performance. The filter performance will provide a benchmark to evaluate the overall tracking and data association algorithm of phase 2.
2. **Phase 2:** Develop the maximum likelihood formulation of the data association problem and solve the resulting problem using a sliding window 2-dimensional assignment algorithm[1] developed at UConn. In this phase the established tracks are associated with the new measurements from the latest scan — this is a 2-dimensional assignment problem.

In this report, we present the results and a software tool termed MATSurv — Multisensor Air Traffic Surveillance System for tracking multiple targets using measurements from asynchronous sensors.

[1]The near optimal association obtained using the 2D-assignment algorithm for the measurement database provided, makes it unnecessary to use the more general S-dimensional algorithm at this juncture. The S-dimensional algorithm has to be used in more complex situations which have crossing, splitting and merging tracks.

2 Description of the Multisensor Data

In this section a description of the *raw scan data* to be used by the *sensor fusion processor*, which gathers and organizes the data from several sensors, is presented.

- The data from the fusion processor consists of scans from two L-band FAA radars located at Remsen("R"), and Dansville("D"), NY.
- The data from two FAA radars consist of scans at approximately every 10 seconds. Each of these scans contains a number of primary radar or *skin* returns. Each of these skin returns consists of a time stamp, a slant range and azimuth angle measurements. For *cooperative* targets a secondary or beacon return is also obtained, which provides, in addition to the above, a target identification number (squawk) and a target altitude measurement.
- The observability of the target state requires a full measurement of its position. Only beacon returns provide such a measurement of the full target position. All the skin returns provide only a partial measurement of the target state, and hence are not used in the tracking filter at the present stage.

The beacon returns also provide the target ID. We make use of this information as follows:

1. In the first phase of the project, all the measurements are associated with the appropriate targets based on the target ID, and the performance of the tracking filter is evaluated. This phase helps to validate and fine tune the filter performance.
2. The availability of the ID of the measurements provides a means for evaluating the performance of the overall algorithm (which involves both association and tracking) in phase 2.

Figure 1 shows the entire data set of measurements with ID, available from the two FAA radars.

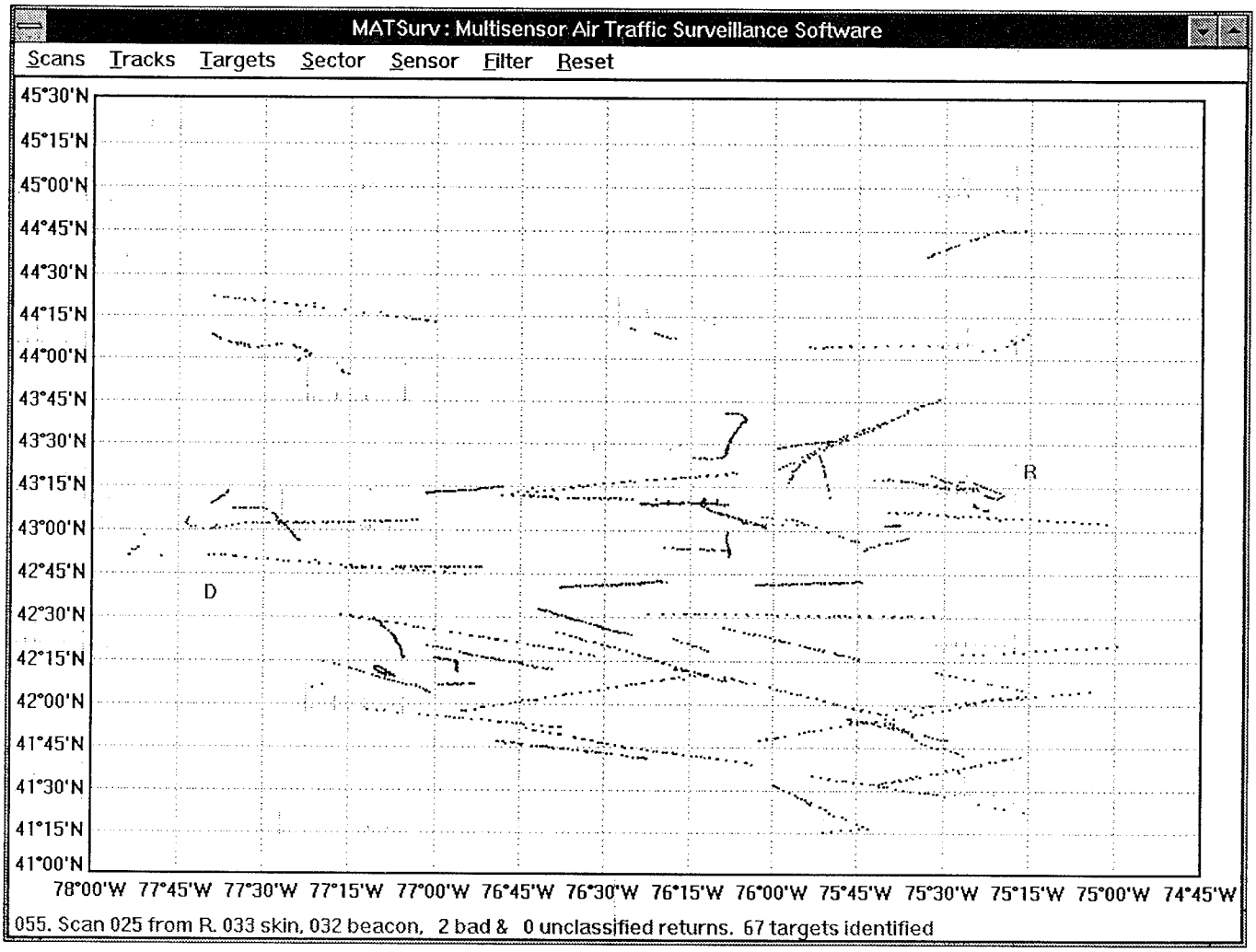

Figure 1: Raw measurements from sites D and R

3 The Sensor Measurement Statistics

The measurement noises of the sensors are assumed to be zero-mean white with variances as follows.

For the range, the resolution cells are

$$\Delta r = \frac{c\tau}{2}, \tag{1}$$

where $c = 3 \cdot 10^8\ m/s$ and τ is the pulse width (6 μs for Remsen and 1.8 μs for Dansville). It is assumed that the range measurement is uniformly distributed in each resolution cell, hence the standard deviation of the range measurement noise is $\sigma_r = \frac{\Delta r}{\sqrt{3}}$, which yields $0.5196\ km = 0.2806\ nmi$ for Remsen and $0.1559\ km = 0.0842\ nmi$ for Dansville.

The azimuth measurement noise standard deviations were taken as $\sigma_\theta = 2.618\ mrad = 0.15°$ based on FAA data. No other specific information was available.

The altitude measurement noise was taken, based on FAA data, as

$$\sigma_h = \sqrt{50^2 + \frac{100^2}{12}} = 57.7350\ ft = 17.5976\ m$$

4 Design of the Tracking Filter

A description of the design and implementation details of the tracking filter is given below. The overall block diagram of this filter is shown in Figure 2.

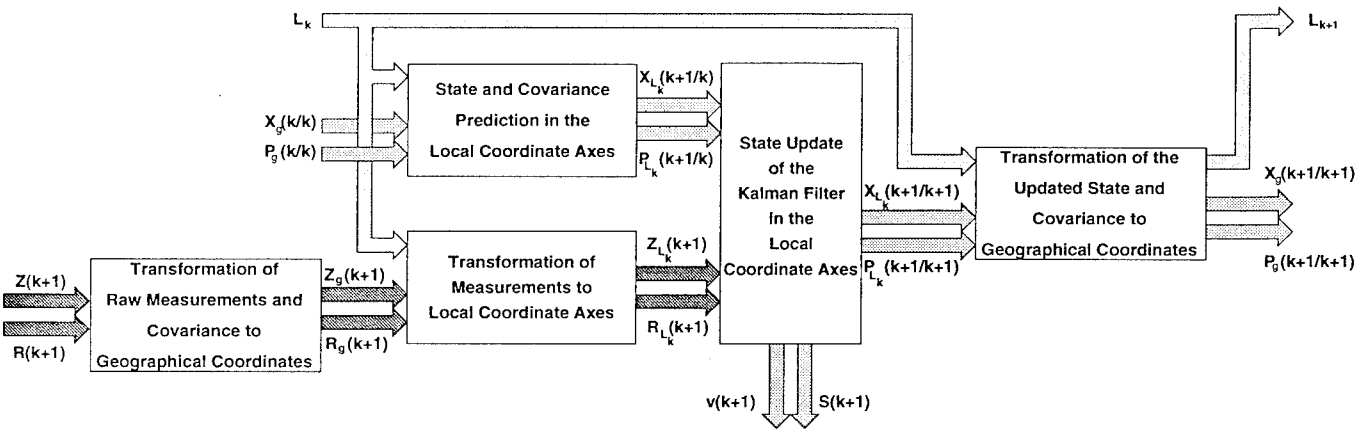

Figure 2: Block diagram of the tracking filter with conversions between three coordinate systems (sensor, target-local and the global).

The following steps in the tracking filter design are described:

- The scenario of interest cannot be modeled as linear both due to the nonlinearity of measurement equations as well as to the large geographical area involved. The latter makes it necessary to use a spherical earth model in place of a flat earth approximation.

- In order to be able to apply the standard Kalman filter, we need a three dimensional Cartesian coordinate frame of reference. In addition, the instantaneous target motion in this frame of reference is approximated by a linear model.

- We start the description of the tracking filter after the k^{th} sampling interval. The estimated target state in geographical coordinates $\mathbf{x}_g(k|k)$ is a 8×1 vector with the following components:

$$\mathbf{x}_g(k|k) = \begin{bmatrix} x_\psi(k|k) & \text{- latitude, } [-\pi/2,\ \pi/2] \\ x_\lambda(k|k) & \text{- longitude, } [-\pi,\ \pi] \\ x_a(k|k) & \text{- altitude in km (above MSL)} \\ \dot{x}_\psi(k|k) & \text{- velocity due north in km/s} \\ \dot{x}_\lambda(k|k) & \text{- velocity due east in km/s} \\ \dot{x}_a(k|k) & \text{- vertical velocity up in km/s} \\ \ddot{x}_\psi(k|k) & \text{- acceleration due north in km/s}^2 \\ \ddot{x}_\lambda(k|k) & \text{- acceleration due east in km/s}^2 \end{bmatrix} \tag{2}$$

- As can be seen from the above definition, the state estimate $\mathbf{x}_g(k|k)$ is in mixed dimensions (i.e., in angles and distances). Nevertheless, we define the covariance matrix $P_g(k|k)$ completely in terms of distance and distance rates only. The compatibility between the state in mixed dimensions and the covariance in uniform dimensions can be understood by interpreting latitude as *distance due north of equator* and longitude as *distance due east of Greenwich meridian.* We can thereby define $P_g(k|k)$ as the covariance matrix associated with the distance errors due north, east and up and errors in their corresponding time derivatives.

- A "local Cartesian coordinate frame" is defined based on the target state estimate $\mathbf{x}_g(k|k)$. The origin of this reference frame is $[x_\psi(k|k) \quad x_\lambda(k|k) \quad 0]$ and the axes are oriented along the north $\mathbf{n}_k$, east $\mathbf{e}_k$, and altitude $\mathbf{u}_k$ directions. The symbol L_k is used to denote this local reference frame uniquely defined by the origin and the three coordinate axes.

- The raw measurement $\mathbf{z}(k+1)$ vector (consisting of slant range, azimuth and altitude) is first transformed into the geographical coordinates $\mathbf{z}_g(k+1)$. The three components of $\mathbf{z}_g(k+1)$ are the latitude, longitude and altitude. The raw measurement covariance $R(k+1)$ is transformed to $R_g(k+1)$ via the first order approximation: $R_g = \left[\nabla_{\mathbf{z}} \mathbf{z}_g'\right] R \left[\nabla_{\mathbf{z}} \mathbf{z}_g'\right]'$. The Jacobian $\nabla_{\mathbf{z}} \mathbf{z}_g'$ is evaluated at the raw measurement $\mathbf{z}(k+1)$.

- The measurement $\mathbf{z}_g(k+1)$ and covariance $R_g(k+1)$ are transformed into the local Cartesian axes L_k. This transformation yields $\mathbf{z}_{L_k}(k+1)$ and $R_{L_k}(k+1)$. Note that the measurement $\mathbf{z}_g(k+1)$ is in mixed dimensions (two angles and one distance) whereas $\mathbf{z}_{L_k}(k+1)$ consists of all distance components. A similar mapping occurs in the transformation of the measurement covariance matrix from $R_g(k+1)$ to $R_{L_k}(k+1)$.

- The geographical state estimate $\mathbf{x}_g(k|k)$ and covariance $P_g(k|k)$ are mapped into the local coordinate axes L_k. This yields $\mathbf{x}_{L_k}(k|k)$ and $P_{L_k}(k|k)$ as:

$$\mathbf{x}_{L_k}(k|k) = \left[\begin{array}{cccccccc} 0 & 0 & x_a(k|k) & \dot{x}_\psi(k|k) & \dot{x}_\lambda(k|k) & \dot{x}_a(k|k) & \ddot{x}_\psi(k|k) & \ddot{x}_\lambda(k|k) \end{array}\right]' \tag{3}$$

$$P_{L_k}(k|k) = P_g(k|k) \tag{4}$$

The predicted state $\mathbf{x}_{L_k}(k+1|k)$ and covariance $P_{L_k}(k+1|k)$ are determined by assuming that the instantaneous target motion is linear along the local coordinate axes L_k.

$$\mathbf{x}_{L_k}(k+1|k) = \Phi_k \mathbf{x}_{L_k}(k|k) \tag{5}$$

$$P_{L_k}(k+1|k) = \Phi_k \, P_{L_k}(k+1|k) \, \Phi_k' + \Gamma_k \, Q_k \, \Gamma_k' \tag{6}$$

- The system matrices are given by

$$\Phi_k = \begin{bmatrix} 1 & 0 & 0 & \delta_k & 0 & 0 & \frac{1}{2}\delta_k^2 & 0 \\ 0 & 1 & 0 & 0 & \delta_k & 0 & 0 & \frac{1}{2}\delta_k^2 \\ 0 & 0 & 1 & 0 & 0 & \delta_k & 0 & 0 \\ 0 & 0 & 0 & 1 & 0 & 0 & \delta_k & 0 \\ 0 & 0 & 0 & 0 & 1 & 0 & 0 & \delta_k \\ 0 & 0 & 0 & 0 & 0 & 1 & 0 & 0 \\ 0 & 0 & 0 & 0 & 0 & 0 & 1 & 0 \\ 0 & 0 & 0 & 0 & 0 & 0 & 0 & 1 \end{bmatrix}, \quad \Gamma_k = \begin{bmatrix} \frac{1}{2}\delta_k^2 & 0 & 0 \\ 0 & \frac{1}{2}\delta_k^2 & 0 \\ 0 & 0 & \frac{1}{2}\delta_k^2 \\ \delta_k & 0 & 0 \\ 0 & \delta_k & 0 \\ 0 & 0 & \delta_k \\ 1 & 0 & 0 \\ 0 & 1 & 0 \end{bmatrix} \tag{7}$$

and $\delta_k = t_{k+1} - t_k$ is the sampling time interval[2]. The process noise covariance matrix Q_k is of the form

$$Q_k = \begin{bmatrix} \sigma_n^2(k) & 0 & 0 \\ 0 & \sigma_e^2(k) & 0 \\ 0 & 0 & \sigma_a^2(k) \end{bmatrix} \tag{8}$$

- The choice of $\sigma_n(k)$, $\sigma_e(k)$ and $\sigma_u(k)$ is a critical design issue. Since $\sigma_n(k)$ and $\sigma_e(k)$ are process noise levels along north and east axes, they are set to the same value, i.e., $\sigma_n(k) = \sigma_e(k) = \sigma_h(k)$ where h denotes horizontal. The vertical motion of the target is *more predictable* than along the horizontal axes. Hence, the process noise level along the altitude axes $\sigma_a(k)$ is different from $\sigma_h(k)$. Both the horizontal, $\sigma_h(k)$, and the altitude, $\sigma_a(k)$, process noise levels are chosen according to the graph shown in Figure 3.

[2]The time interval δ_k can in general be negative, particularly when the detection at t_{k+1} and the detection at t_k originate from different radars. The implementation of the filter for negative time updates is explained in the appendix.

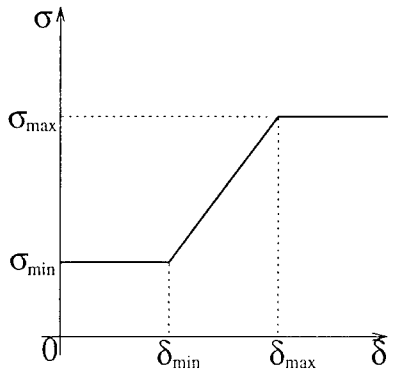

Figure 3: Process Noise Level as a function of Sampling Interval

- For $\sigma_h(k)$ we chose

$$\sigma_{h_{\max}} = 7.5\ m/s^2 \qquad \sigma_{h_{\min}} = 0.0\ m/s^2$$

$$\delta_{h_{\min}} = 0.0\ s \qquad \delta_{h_{\max}} = 40.0\ s$$

and for $\sigma_a(k)$ the following values were chosen

$$\sigma_{a_{\max}} = 0.5\ m/s^2 \qquad \sigma_{a_{\min}} = 0.0\ m/s^2$$

$$\delta_{a_{\min}} = 1.0\ s \qquad \delta_{a_{\max}} = 40.0\ s$$

- The linear Kalman filter state and covariance update equations are implemented in the local Cartesian coordinates. These update equations yield $\mathbf{x}_{L_k}(k+1|k+1)$ and $P_{L_k}(k+1|k+1)$. In addition we get the innovations $\nu_{L_k}(k+1)$ and the innovations covariance $S_{L_k}(k+1)$ which are used to gauge the performance of the filter.

$$\begin{aligned}
\nu_{L_k}(k+1) &= \mathbf{z}_{L_k}(k+1) - H\,\mathbf{x}_{L_k}(k+1|k) && (9)\\
S_{L_k}(k+1) &= H\,P_{L_k}(k+1|k)\,H' + R_{L_k}(k+1) && (10)\\
W_{L_k}(k+1) &= P_{L_k}(k+1|k)\,H'\,S_{L_k}(k+1)^{-1} && (11)\\
\mathbf{x}_{L_k}(k+1|k+1) &= \mathbf{x}_{L_k}(k+1|k) + W_{L_k}(k+1)\,\nu_{L_k}(k+1) && (12)\\
P_{L_k}(k+1|k+1) &= P_{L_k}(k+1|k) - W_{L_k}(k+1)\,S_{L_k}(k+1)\,W_{L_k}(k+1)' && (13)
\end{aligned}$$

where $H = [I\ 0\ 0]_{3\times 8}$ and the 8×3 matrix $W_{L_k}(k+1)$ is the filter gain.

- The updated state $\mathbf{x}_{L_k}(k+1|k+1)$ and covariance $P_{L_k}(k+1|k+1)$ are along the L_k reference frame. To complete the cycle of transformations, we transform the updated state $\mathbf{x}_{L_k}(k+1|k+1)$ and covariance $P_{L_k}(k+1|k+1)$ into geographical coordinates $\mathbf{x}_g(k+1|k+1)$ and $P_g(k+1|k+1)$, respectively. The two equations below illustrate the sequence of operations that are involved in this transformation.

$$\begin{aligned}
\mathbf{x}_{L_k}(k+1|k+1) &\overset{L_k}{\Longrightarrow} \mathbf{x}_g(k+1|k+1) \Longrightarrow L_{k+1}\\
P_{L_k}(k+1|k+1) &\overset{L_k,\,L_{k+1}}{\Longrightarrow} \mathbf{x}_g(k+1|k+1),\ P_g(k+1|k+1)
\end{aligned}$$

- The filter is initialized using the first two measurements, i.e., $\mathbf{x}_g(2|2)$ and $P_g(2|2)$ are determined using two point diferencing from $\mathbf{z}_g(1)$, $R_g(1)$ and $\mathbf{z}_g(2)$, $R_g(2)$. Since only two measurements are used the initial acceleration components $\ddot{x}_\psi(2|2)$ and $\ddot{x}_\lambda(2|2)$ are both set to zero.

5 Data Association

In this section we present the formulation and results of the data association problem. A sliding window 2-dimensional assignment algorithm has been used.

The formulation of the 2-D assignment problem is presented below. Consider the scenario at scan $k > 1$. There are $n(k)$ validated tracks from the previous assignments, and corresponding to track i, $i = 1, \cdots, n(k)$, we have the latest state estimate $\mathbf{x}_g^{(i)}(k|k)$ and covariance $P_g^{(i)}(k|k)$. Let scan $k+1$ contain $m(k+1)$ measurements.

The hypotheses upon which the 2-D assignment algorithm is based on are the following:

1. Measurement j, $1 \leq j \leq m(k+1)$ originated from a target corresponding to one of the $n(k)$ validated tracks, say track i, $i = 1, \cdots, n(k)$.

2. Measurement j, $1 \leq j \leq m(k+1)$ is a false alarm. Track index $i = 0$ is used to designate a *dummy target* (i.e., a source of false alarms). Such a measurement is also kept as a candidate for a new track, i.e., if within $T_D = 30s$ it has another measurement in its neighborhood it initiates a new track.

Each track (excluding track 0) is assigned at most one measurement, and each measurement is assigned to at most one track. On the other hand, the number of measurements that may be assigned to track 0 is not limited.

An existing track is dropped if within $T_D = 60s$ no new measurement is associated with it.

5.1 Feasible Assignments

We shall define an assignment ω, as the mapping between the measurement indices j and the track indices i. This assignment can be represented using the set of binary $(0,1)$ variables $\{\rho_{i,j}\}$.

A feasible assignment must satisfy the following requirements

$$\omega = \{\rho_{i,j} \in \{0,1\},\ \ i = 0,\ldots,n(k),\ \ j = 1,\ldots,m(k+1)\} \tag{14}$$

$$\sum_{i=0}^{n(k)} \rho_{i,j} = 1 \qquad j = 1,\ldots,m(k+1) \tag{15}$$

$$\sum_{j=1}^{m(k+1)} \rho_{i,j} = 1 \qquad i = 1,\ldots,n(k) \tag{16}$$

5.2 The 2D Assignment Problem and its Complexity

Let Ω be the set of all feasible assignments, then the total number of feasible assignments, i.e., the cardinality of the set Ω, can be shown to be

$$|\Omega| = \sum_{i=0}^{p} \left(\frac{p!}{i!}\right) C_{p-i}^{q} \tag{17}$$

where $p = \min\{n(k), m(k+1)\}$ and $q = \max\{n(k), m(k+1)\}$.

Let $c_{i,j}$ be the cost incurred in assigning measurement j to track i. The 2-dimensional assignment problem can now be stated simply as finding an optimal assignment ω^* that minimizes the overall cost, i.e.,

$$\omega^* = \arg\min_{\omega\in\Omega} \sum_{i=0}^{n(k)} \sum_{j=1}^{m(k+1)} \rho_{i,j}\, c_{i,j} \tag{18}$$

The number of feasible assignments, $|\Omega|$, is very large even for moderate values of p and q, hence an efficient assignment algorithm is required for solving this problem. The *modified auction algorithm* is ideally suited for solving this 2-dimensional assignment problem. A detailed description of this algorithm can be found in [1].

In the present context of assigning measurements to tracks, the cost criterion $c_{i,j}$ is the negative logarithm of the ratio of the likelihood of measurement j originating from track $i(\neq 0)$ to the likelihood of measurement j originating from track 0 (i.e., the likelihood that measurement j is a false alarm).

The evaluation of $c_{i,j}$ is presented in the following. The likelihood that measurement j, $1 \leq j \leq m(k+1)$, originated from track i, $1 \leq i \leq n(k)$, is given by

$$\Lambda_{i,j}(k+1) = P_D \cdot |2\pi S_{i,j}(k+1)|^{-\frac{1}{2}} \cdot \exp\left\{-\frac{1}{2}\eta_{i,j}(k+1)\right\} \tag{19}$$

where P_D is the probability of detection, $\eta_{i,j}(k+1)$ is the normalized innovation squared given by

$$\eta_{i,j}(k+1) = \nu_{i,j}(k+1)^T \left[S_{i,j}(k+1)\right]^{-1} \nu_{i,j}(k+1) \tag{20}$$

$\nu_{i,j}(k+1)$ is the innovation and $S_{i,j}(k+1)$ the innovation covariance, associated with the track i filter updated with measurement j.

We shall assume that false alarms are uniformly probable in the whole of the surveillance region of volume $\Psi(k+1)$. Since false alarms are assigned to track 0, the likelihood that the measurement j is a false alarm is,

$$\Lambda_{0,j}(k+1) = \frac{1}{\Psi(k+1)} \tag{21}$$

The cost $c_{i,j}$ of assigning measurement j to track i is the negative log-likelihood ratio, given by

$$c_{i,j} = -\log\left[\frac{\Lambda_{i,j}(k+1)}{\Lambda_{0,j}(k+1)}\right] = \frac{1}{2}\eta_{i,j}(k+1) + \log\left(\frac{|2\pi S_{i,j}(k+1)|^{\frac{1}{2}}}{P_D \Psi(k+1)}\right) \tag{22}$$

The following values have been used for the probability of detection P_D and the surveillance region volume of the region in which a candidate false alarm is uniformly distributed:

$$P_D = 0.999 \tag{23}$$

$$\Psi(k+1) = 1000\ km^3 \tag{24}$$

6 Examples

The performance of the tracking filter and the association algorithm is illustrated for two typical target trajectories.

In example 1, the association algorithm perfectly matches the measurement ID data, and hence the output of the tracking filter with ID and with association is quite identical. These results are shown in figures 4–11. Note that the tracking filter, handles the target maneuver (which is a typical landing pattern) successfully.

In example 2 the trajectory formed using the association algorithm is definitely superior to the one formed using IDs. The results for this example are shown in figures 12–23.

This case is unusual because it appears that the ID was changed toward the end of the flight (before landing). The ID-based association came up with 19 measurements while the assignment algorithm obtained the same 19 plus another 6 by which time there was a new ID but the measurements gave a good filter. This shows the superiority of our assignment algorithm over the "ground truth" which has its quirks. Once again note that the tracking filter is quite robust in handling the rather sharp target maneuver.

Example 3 illustrates two very positive aspects of the association algorithm. Firstly the association algorithm drops a measurement that is very noisy (i.e., outlier rejection), thus yielding a better track than that is obtained using the ID. Secondly, its brings in a measurement that has been (incorrectly) assigned an ID corresponding to a different target. Comparing the tracks shown in figures 27 and 28, it can be seen that dropping the outlying measurement definitely improves the track. The normalized innovations squared shown in figures 31 and 32 clearly indicates that the measurement that is dropped is an outlier while the new measurement (with a different ID) definitely belongs to this target. This is a known phenomenon of transponder interference when two aircraft are close. In this case the "ground truth" might not be true (ID codes have been switched due to the interference).

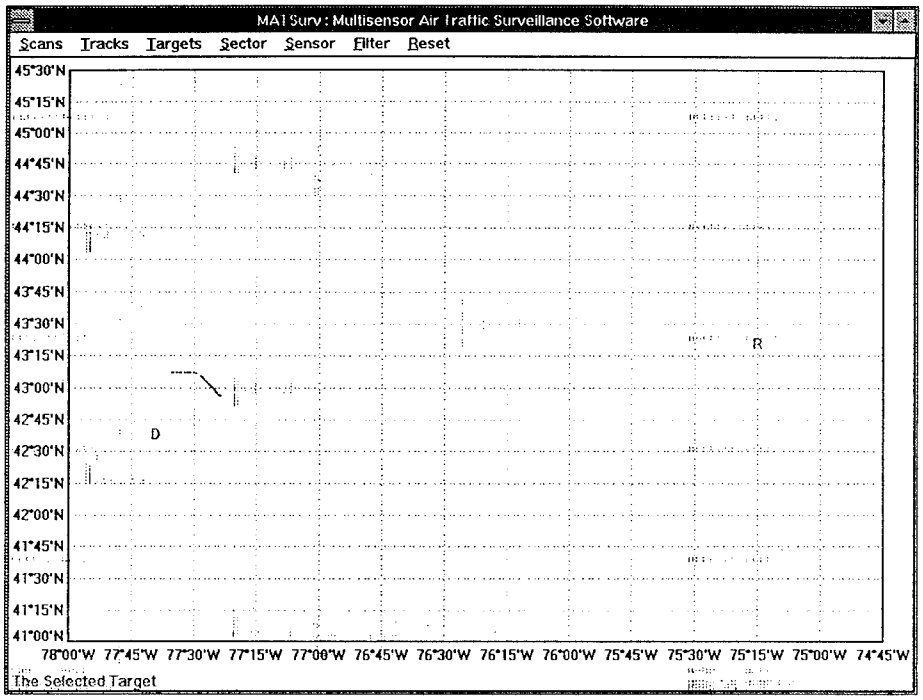

Figure 4: Example 1. Target trajectory, using ID

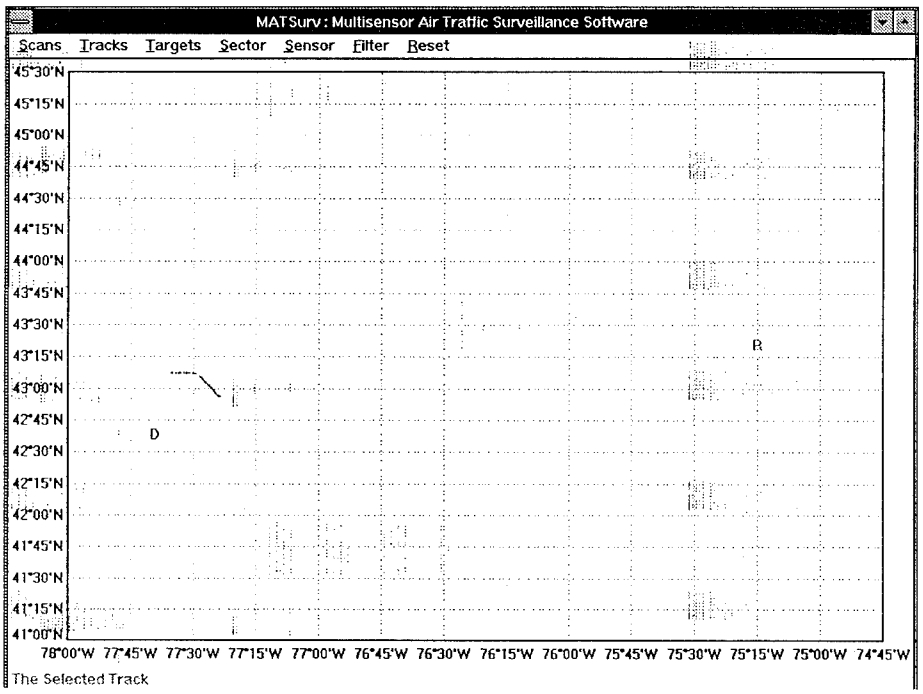

Figure 5: Example 1. Target trajectory, using association (perfectly matches with the IDs)

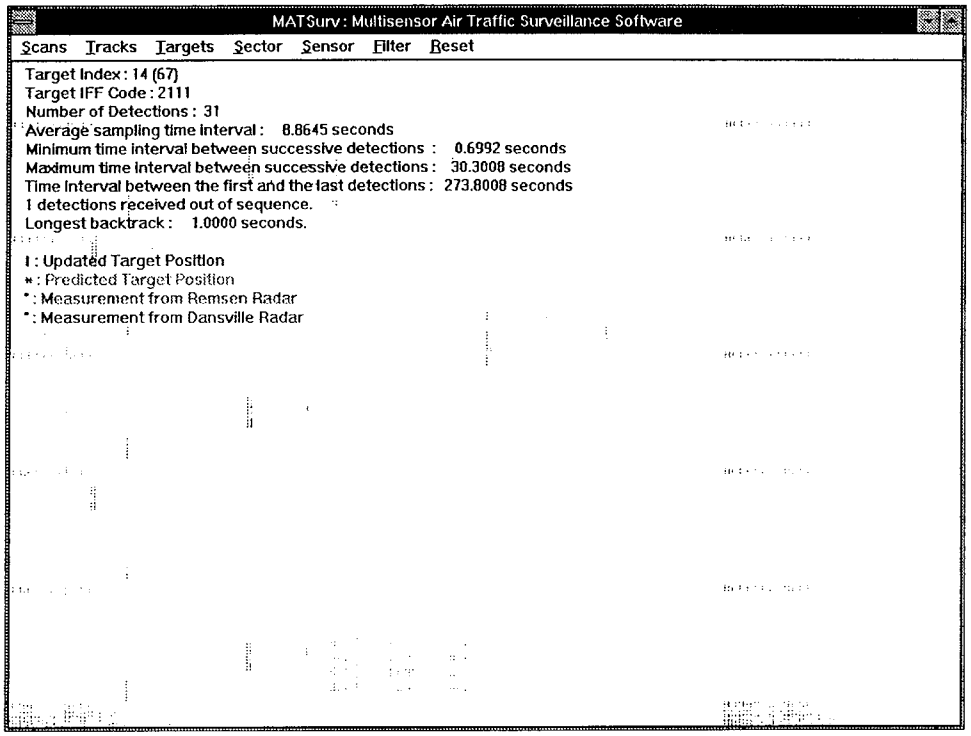

Figure 6: Example 1. Target trajectory information, using ID

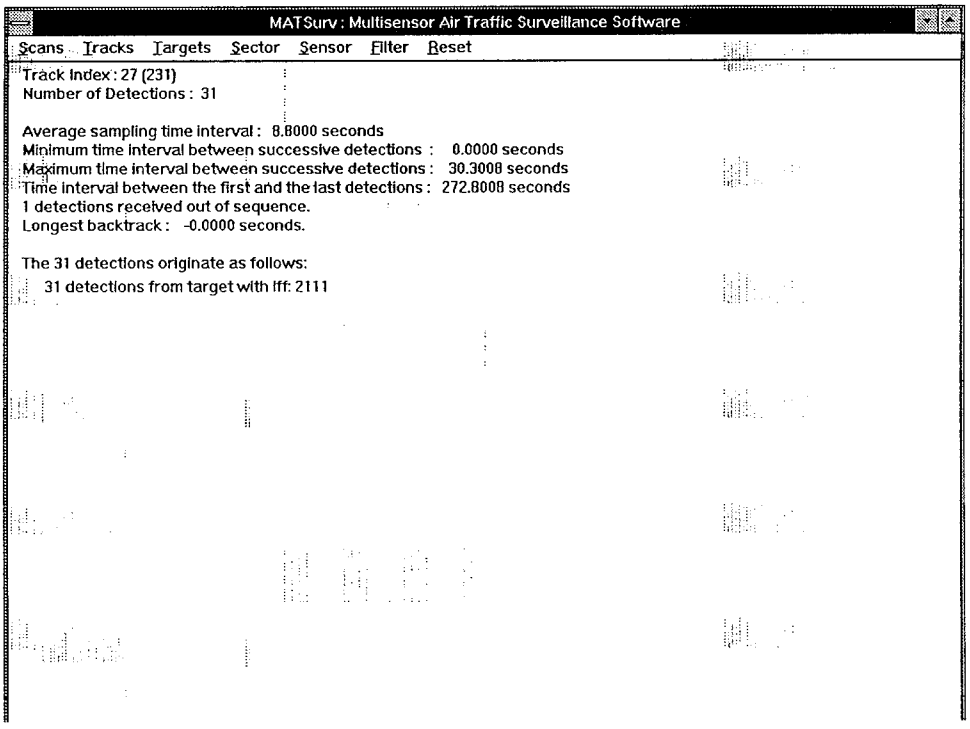

Figure 7: Example 1. Target trajectory information, using association

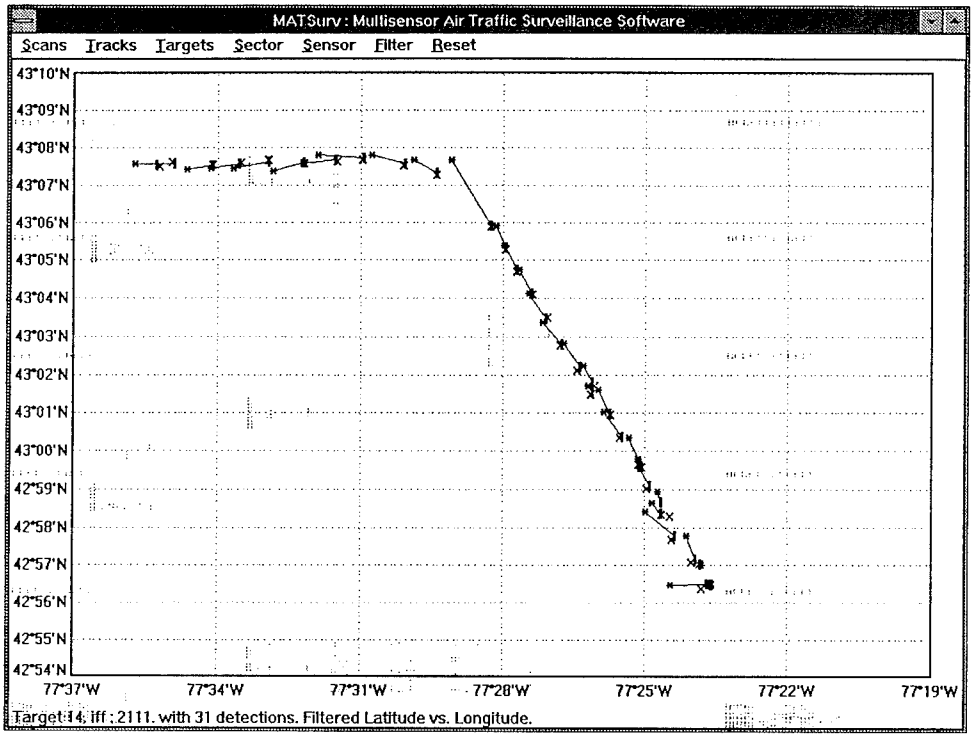

Figure 8: Example 1. Estimated trajectory of target in the horizontal plane

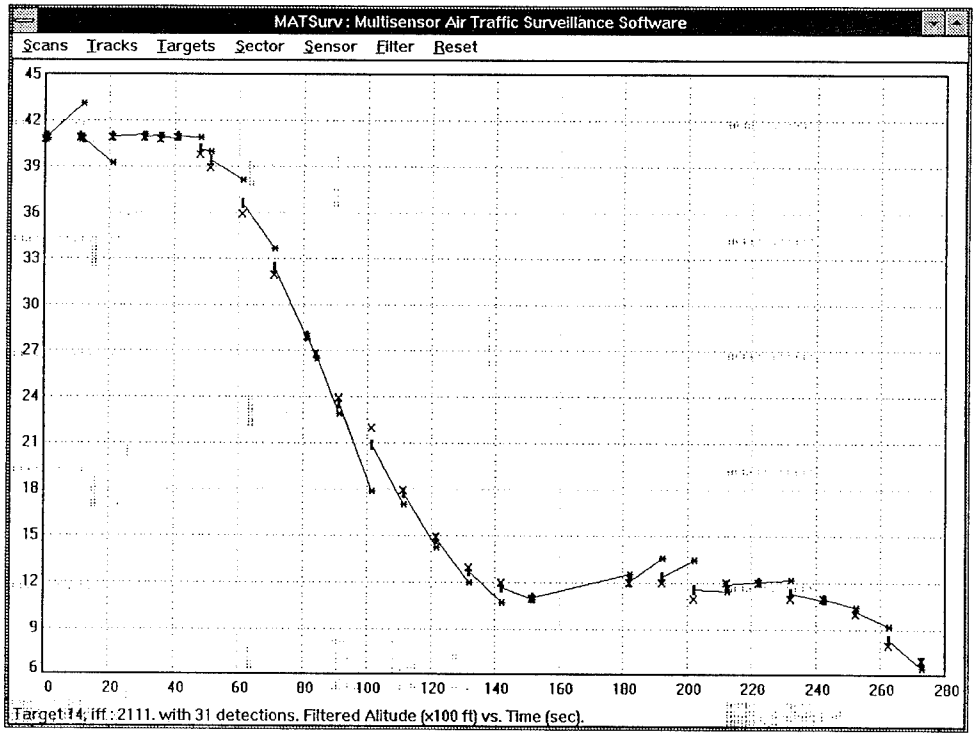

Figure 9: Example 1. Estimated altitude of target

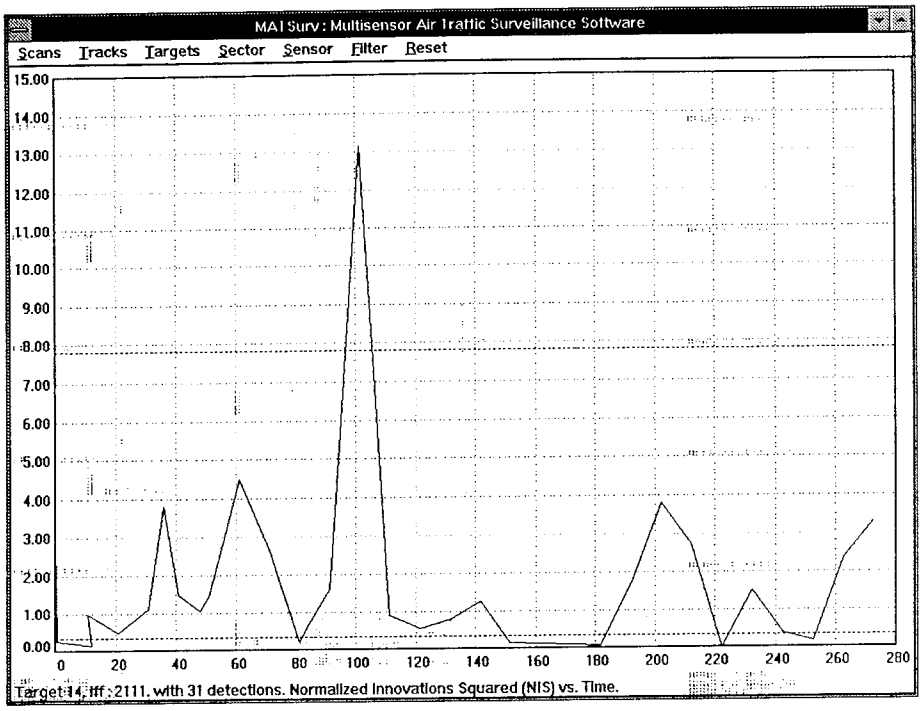

Figure 10: Example 1. Output of tracking filter: Normalized innovation squared (in 3 dimensions)

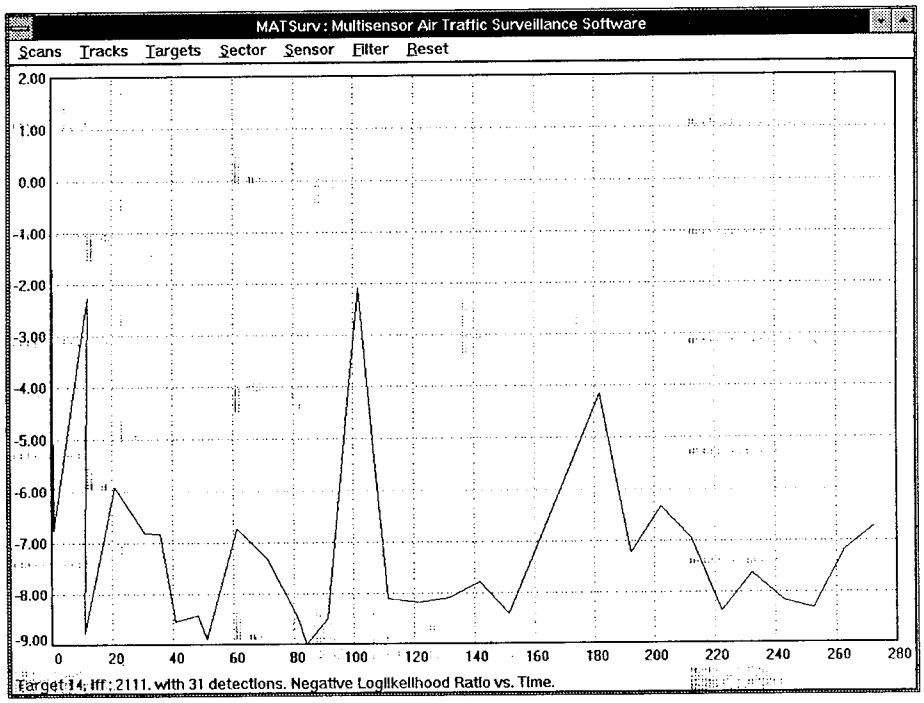

Figure 11: Example 1. Output of tracking filter: Negative log-likelihood ratio (should be below 0 to indicate "target" more likely than "false track")

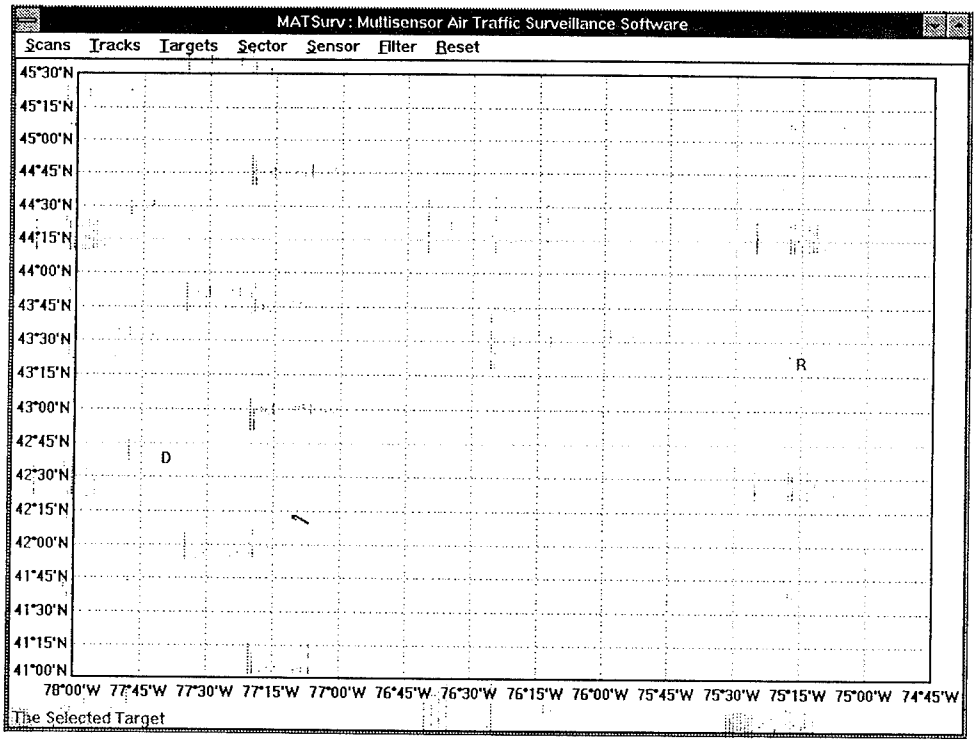

Figure 12: Example 2. Target trajectory classified using ID

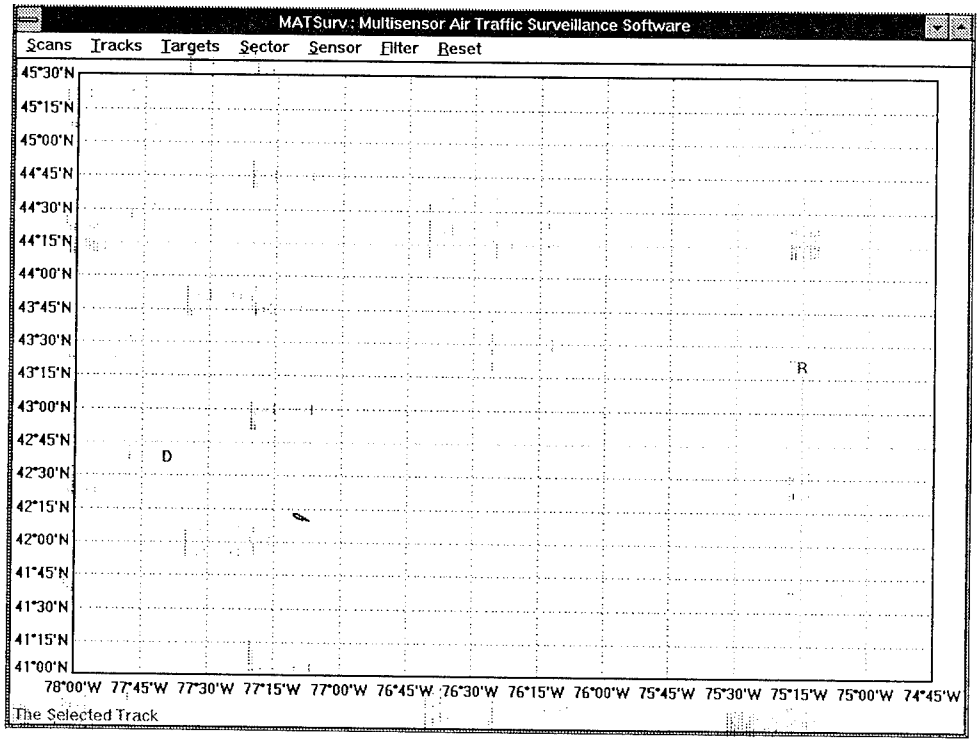

Figure 13: Example 2. Target trajectory using association

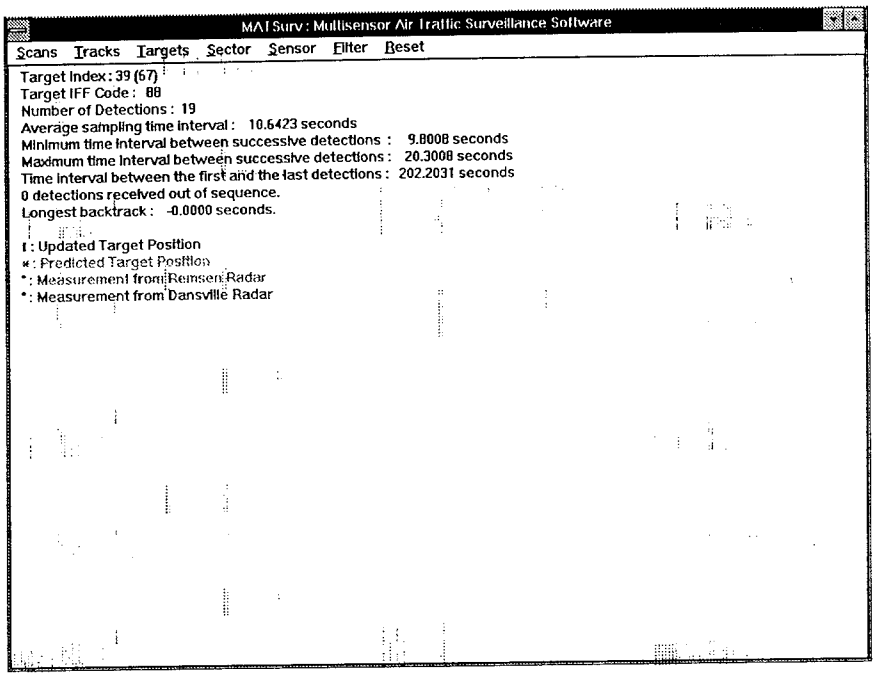

Figure 14: Example 2. Target trajectory information, using ID

Note: 19 detections because ID was changed in flight

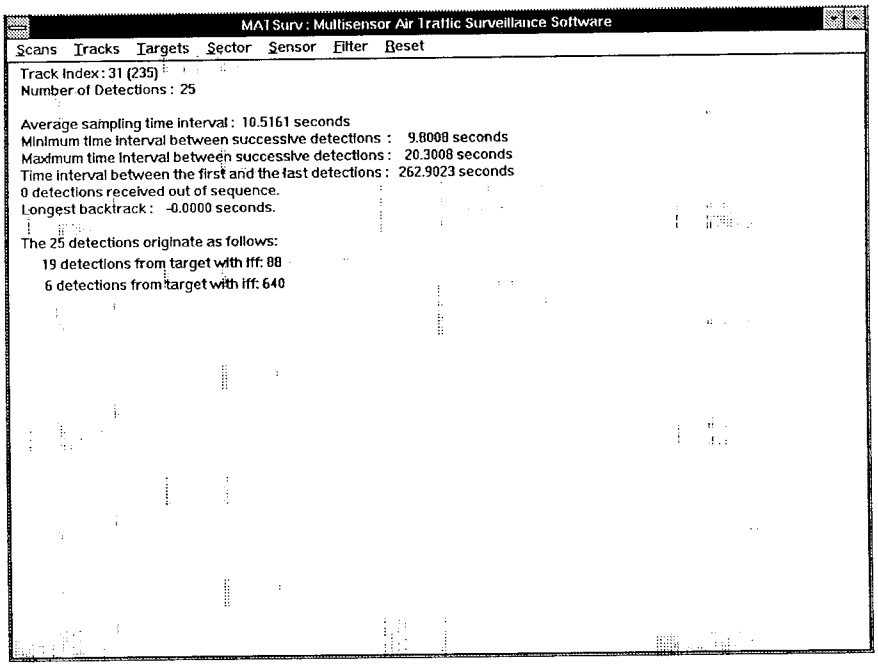

Figure 15: Example 2. Target trajectory information, using association

Note: 25 detections with old & and new ID

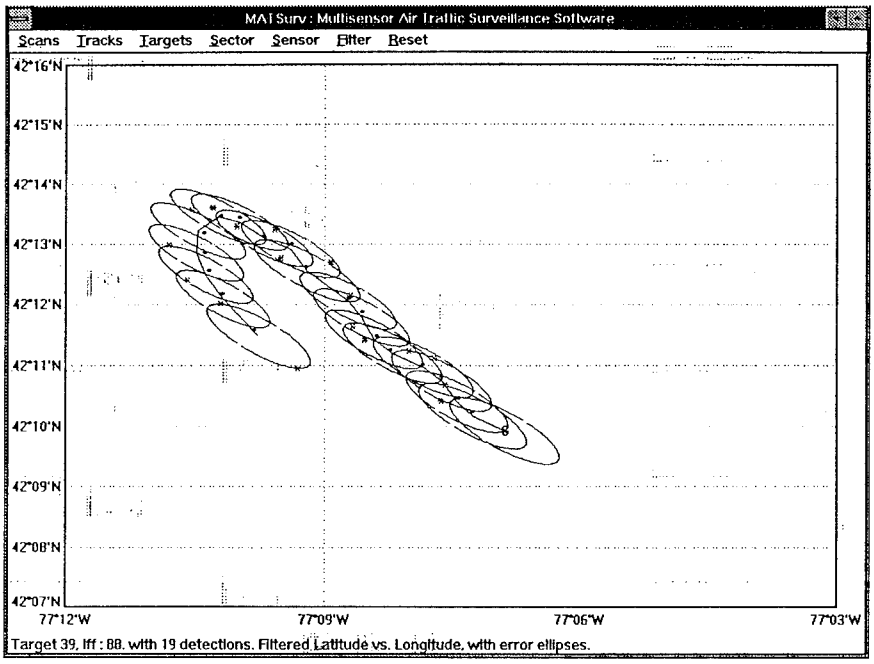

Figure 16: Example 2. Estimated trajectory of target, using ID

(19 detections)

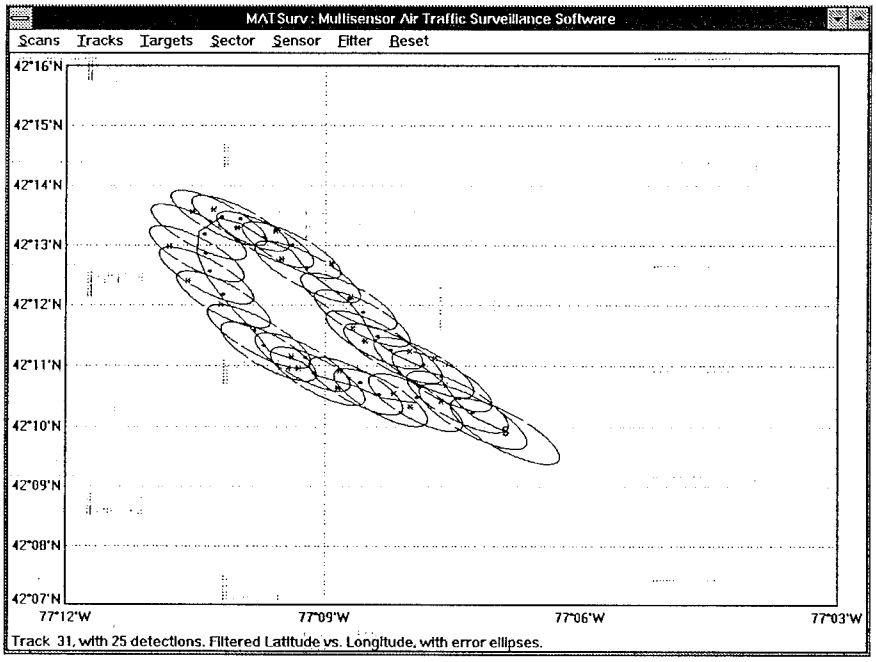

Figure 17: Example 2. Estimated trajectory of target, using association

(25 detections)

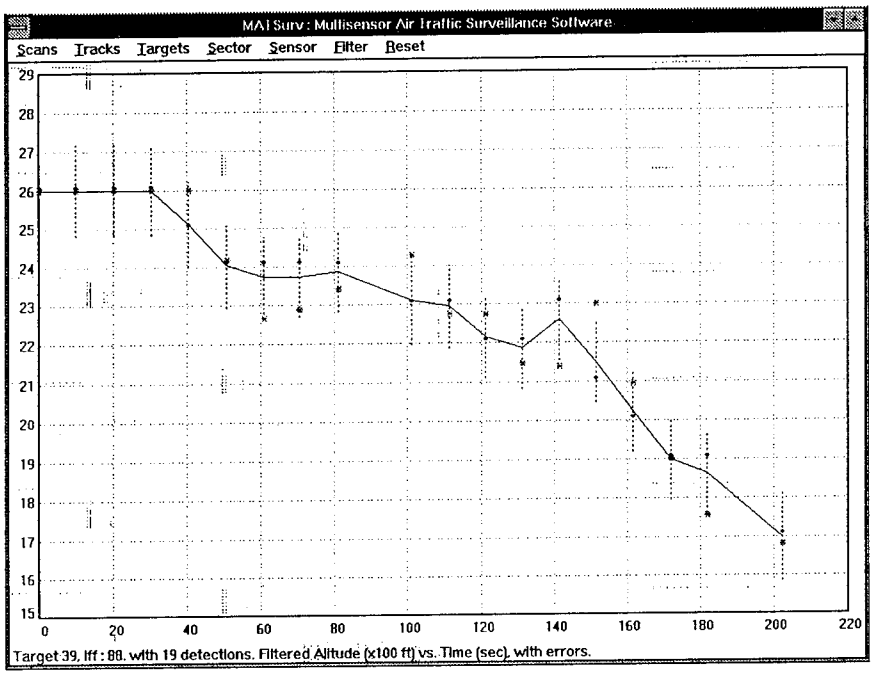

Figure 18: Example 2. Estimated altitude of target, using ID

(19 detections)

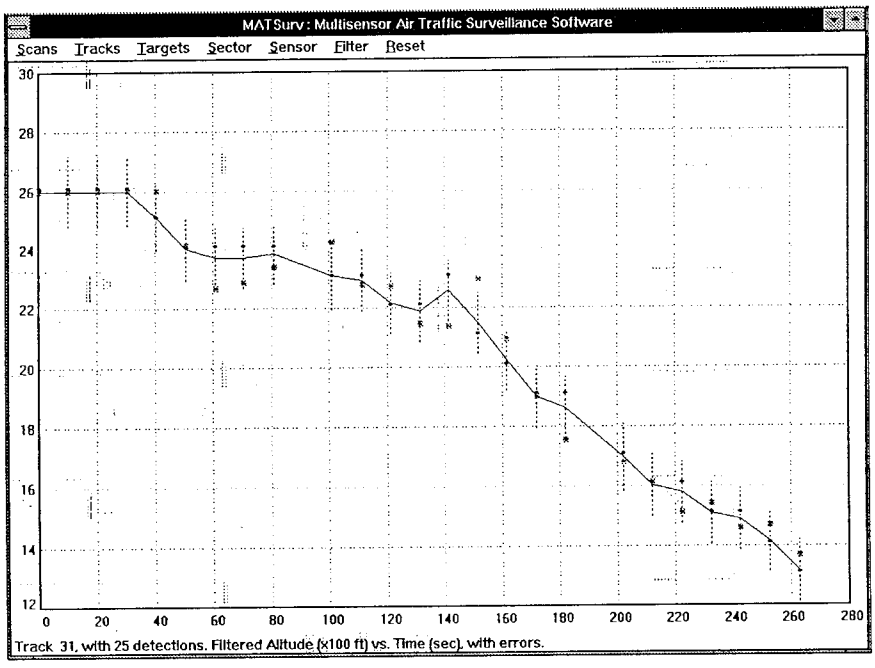

Figure 19: Example 2. Estimated altitude of target, using association

(25 detections)

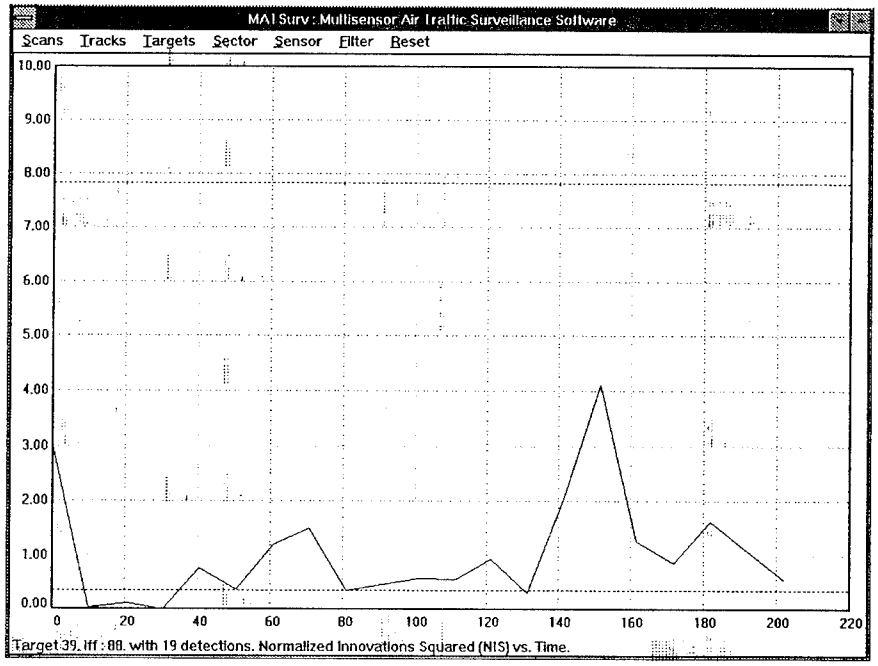

Figure 20: Example 2. Output of tracking filter: Normalized Innovation Squared, using ID

(19 detections)

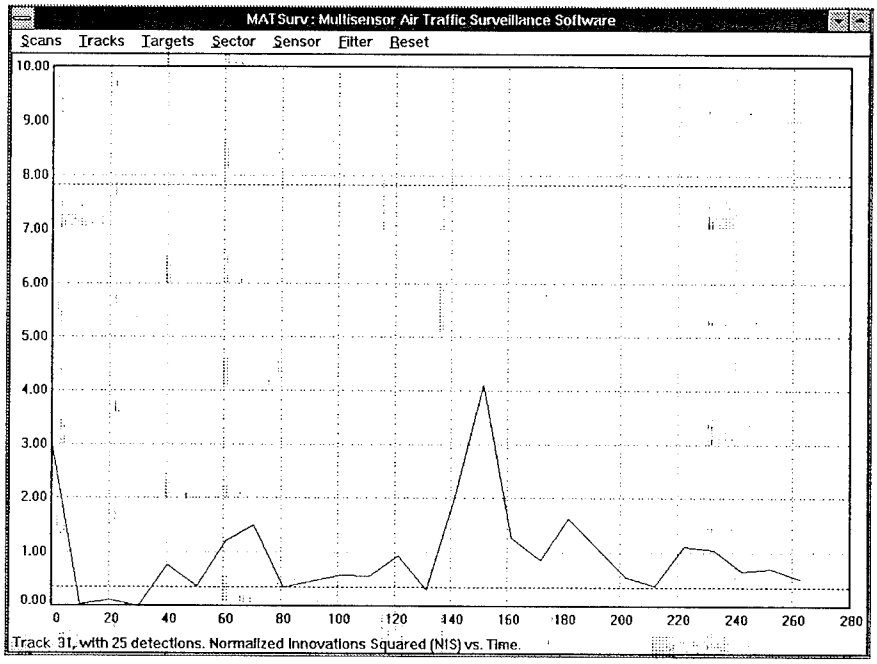

Figure 21: Example 2. Output of tracking filter: Normalized Innovation Squared, using association

(25 detections)

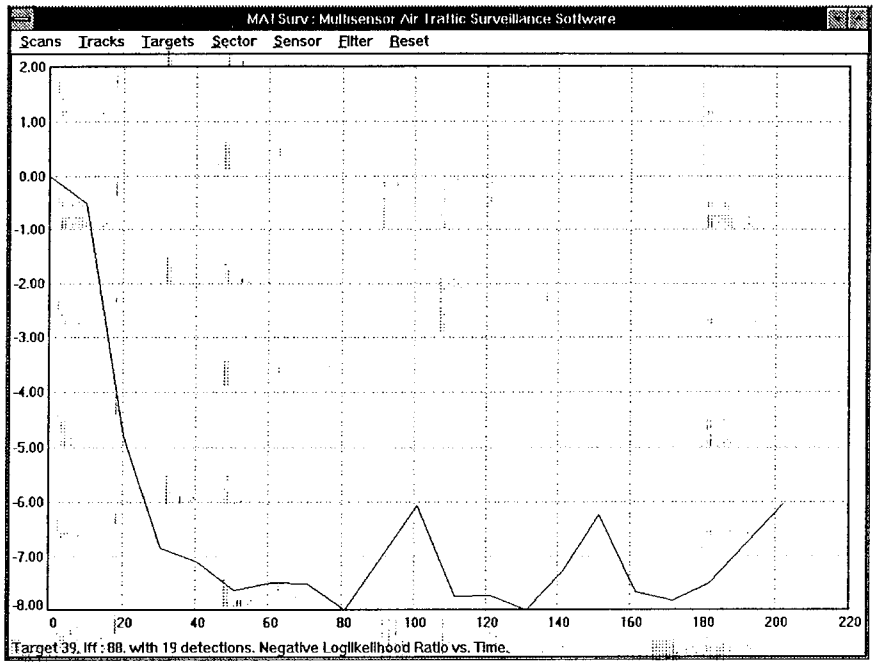

Figure 22: Example 2. Output of tracking filter: Negative log-likelihood ratio, using ID (19 detections)

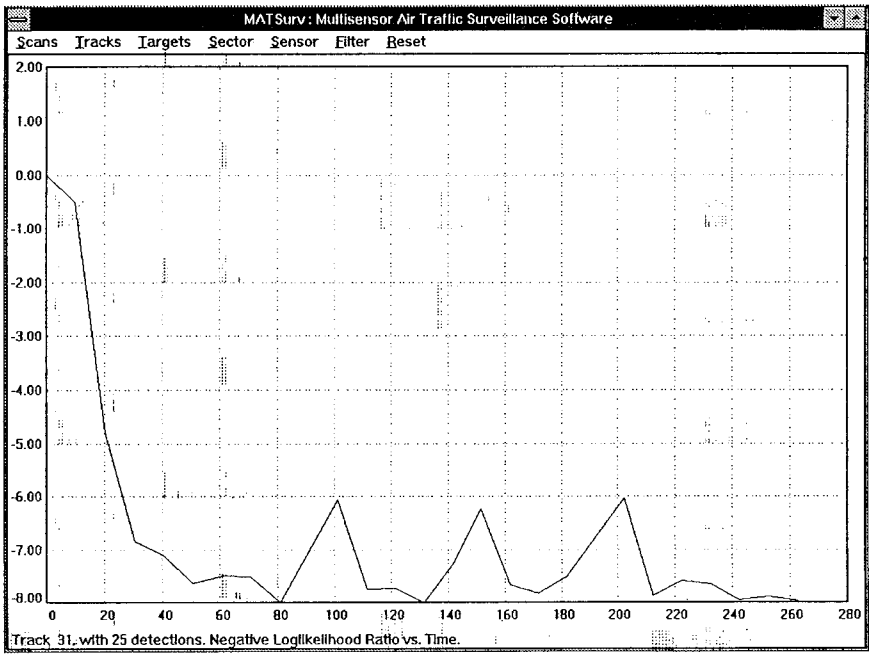

Figure 23: Example 2. Output of tracking filter: Negative log-likelihood ratio, using association (25 detections)

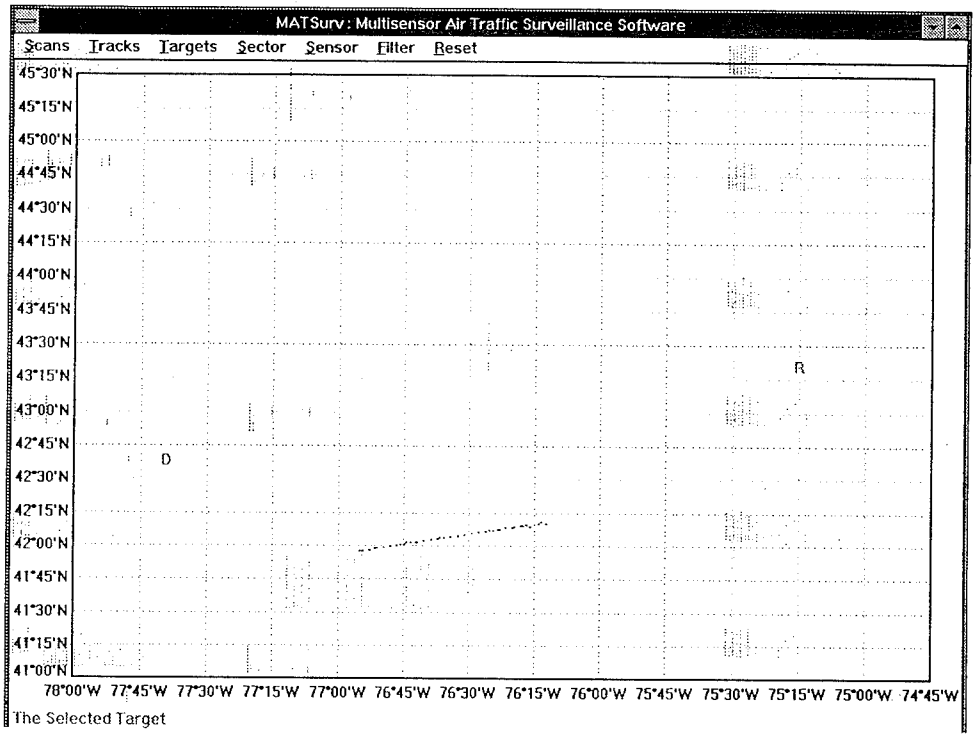

Figure 24: Example 3. Target trajectory classified using ID

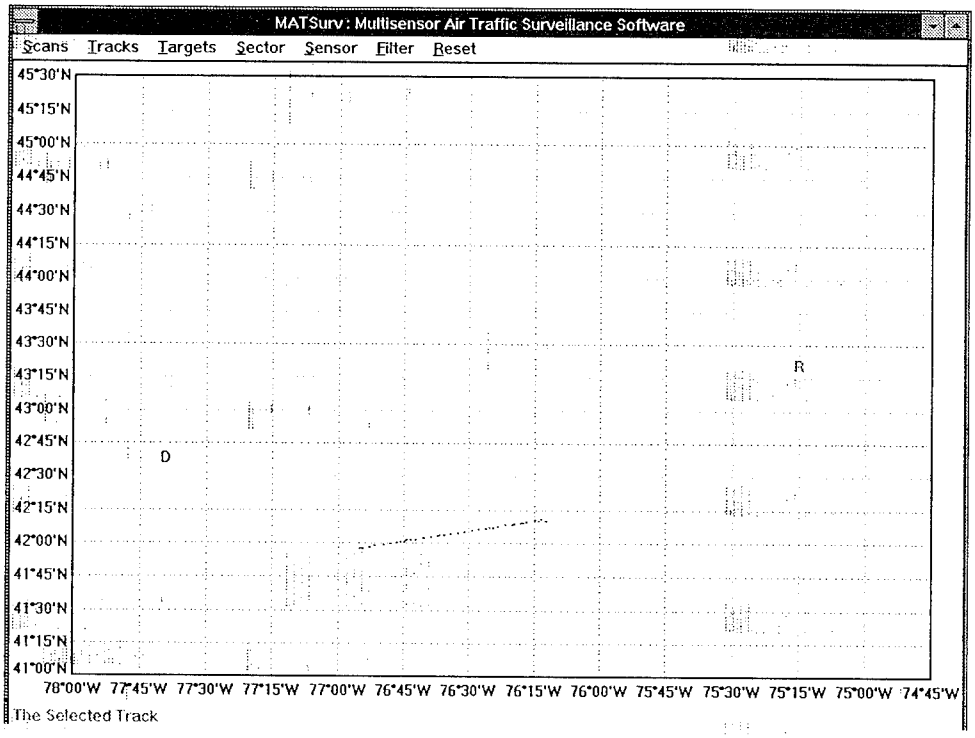

Figure 25: Example 3. Target trajectory using association,

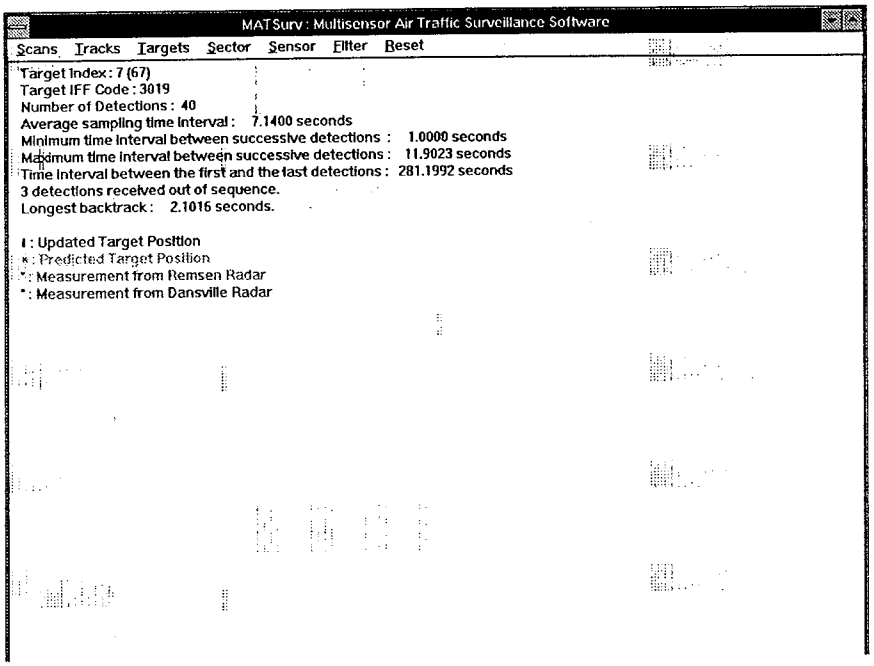

Figure 26: Example 3. Target trajectory information, using ID

40 detections, all detections have the same ID 3019

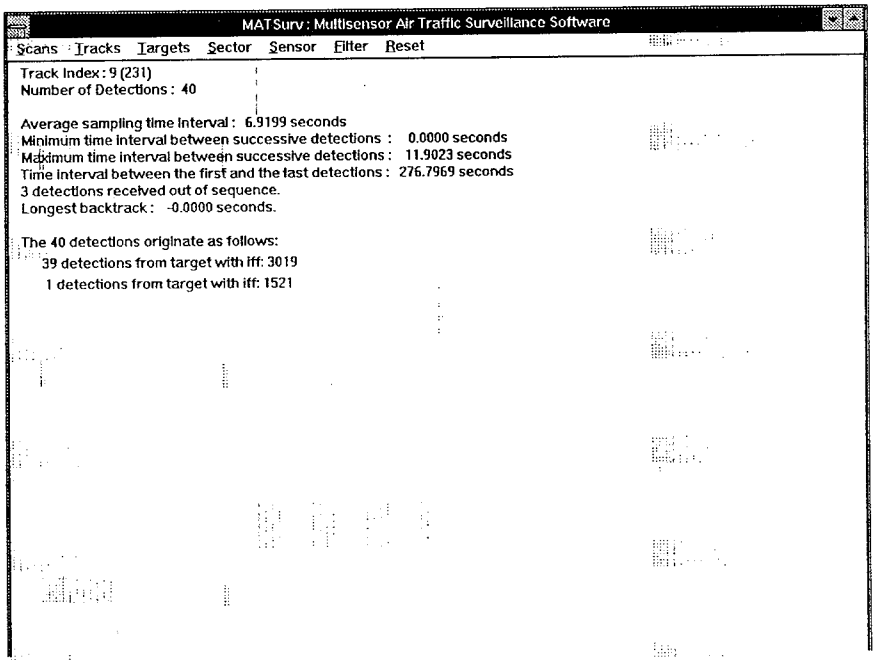

Figure 27: Example 3. Target trajectory information, using association

40 detections: one detection with ID 3019 is discarded, and one detection with ID 1521 is added

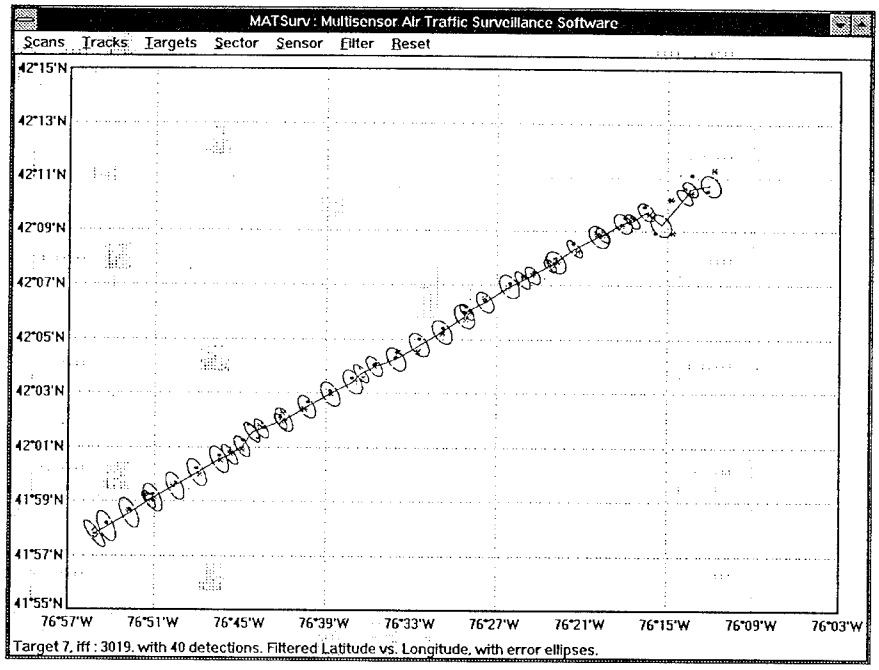

Figure 28: Example 3. Estimated trajectory of target, using ID

Observe the effect of the outlying detection in the top right corner of the track

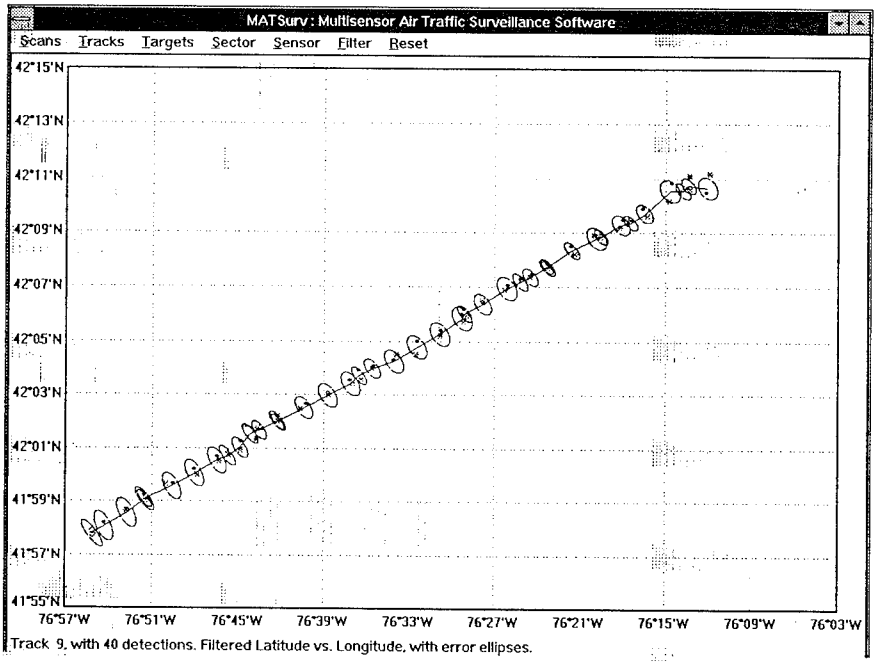

Figure 29: Example 3. Estimated trajectory of target, using association

Notice that the outlying detection (with ID 3019) has been discarded

A new detection (with ID 1521) has been included in the top right corner

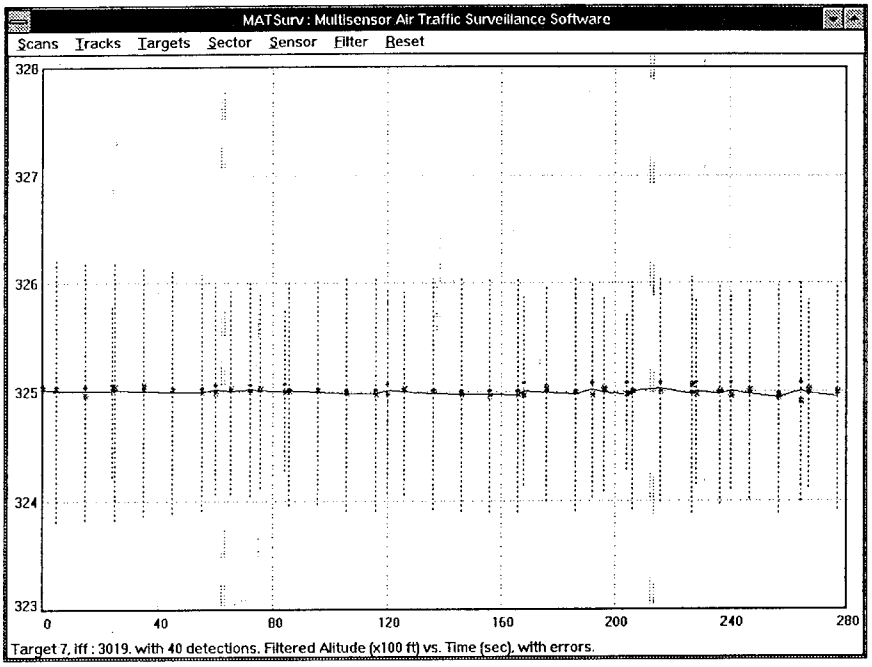

Figure 30: Example 3. Estimated altitude of target, using ID

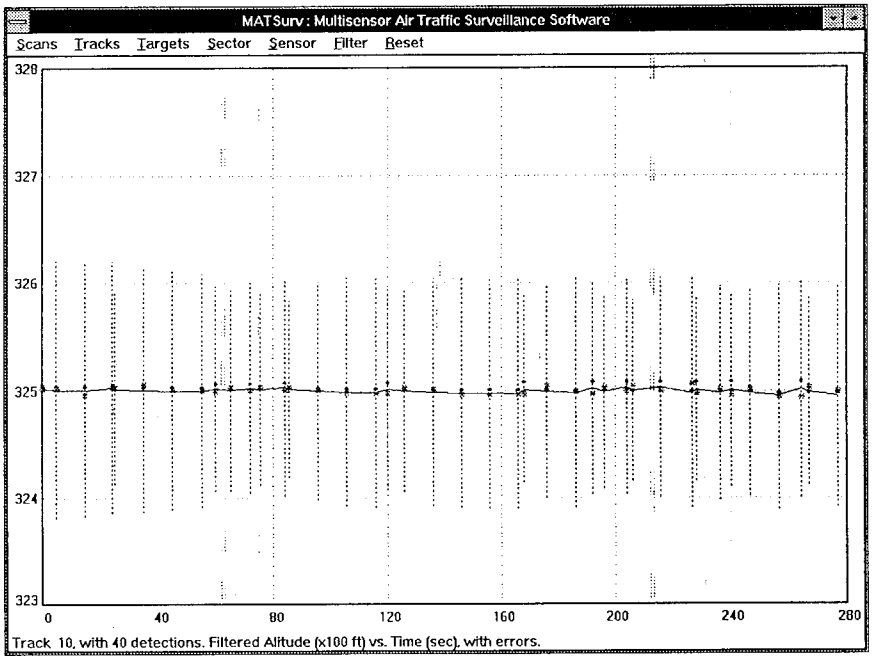

Figure 31: Example 3. Estimated altitude of target, using association

Note that the additional detection (with ID 1521) "conforms" with the rest of the target track

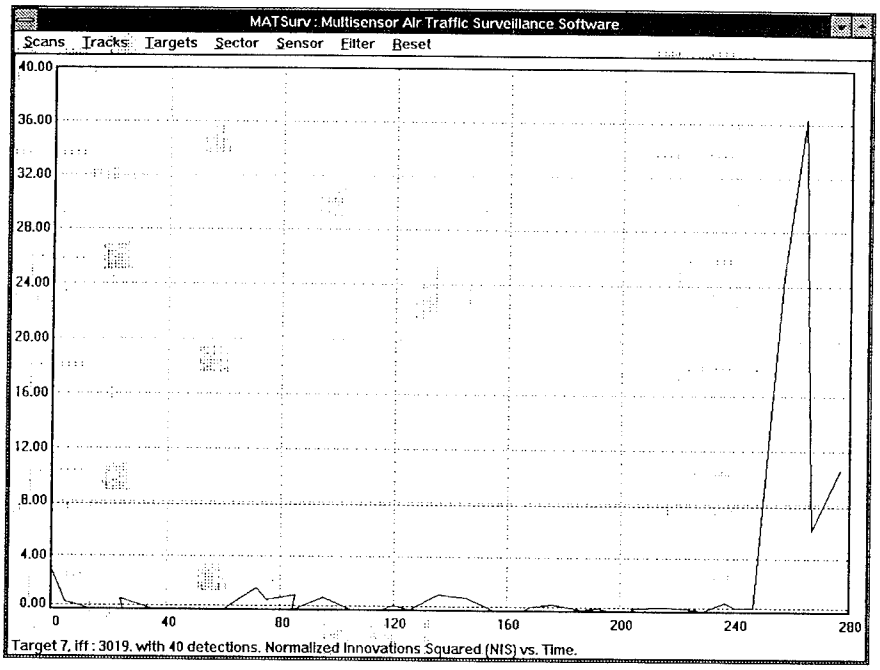

Figure 32: Example 3. Output of tracking filter: Normalized Innovation Squared, using ID

The sharp spike in the NIS is due to the presence of the outlying detection

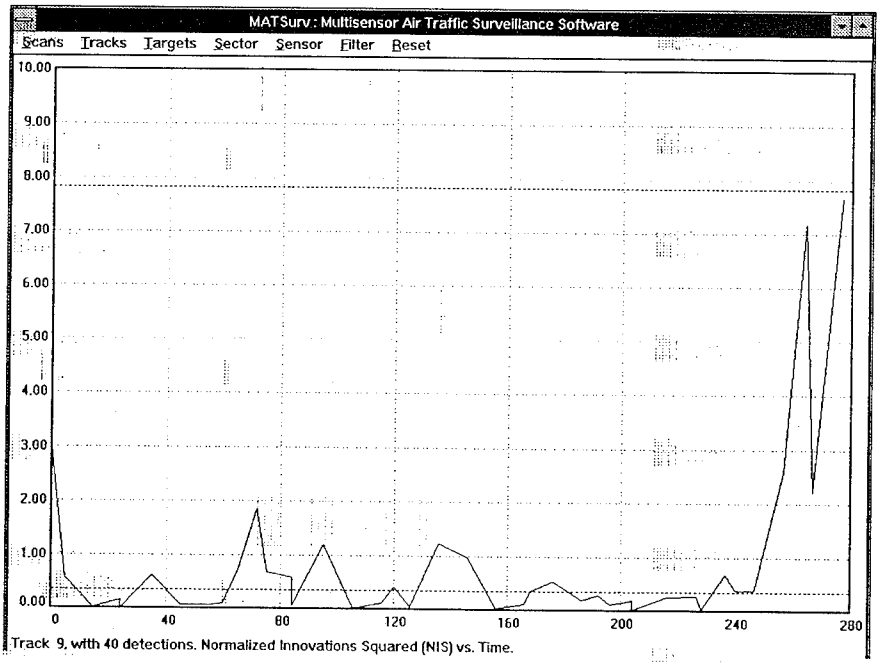

Figure 33: Example 3. Output of tracking filter: Normalized Innovation Squared, using association

Note that the NIS is now within its 95% probability level

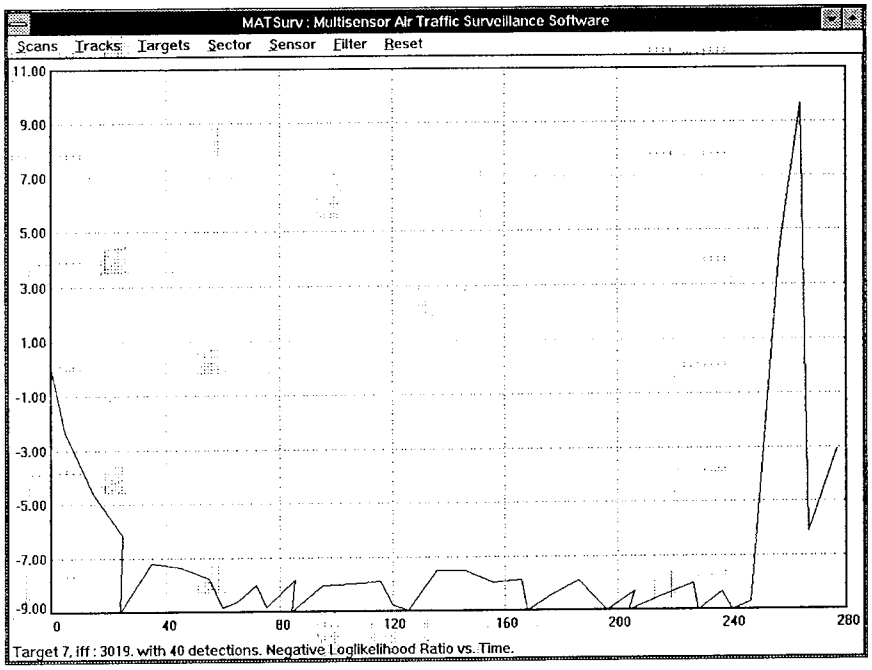

Figure 34: Example 3. Output of tracking filter: Negative log-likelihood ratio, using ID

The outlying detection has a positive log likelihood ratio, hence it is deemed "false"

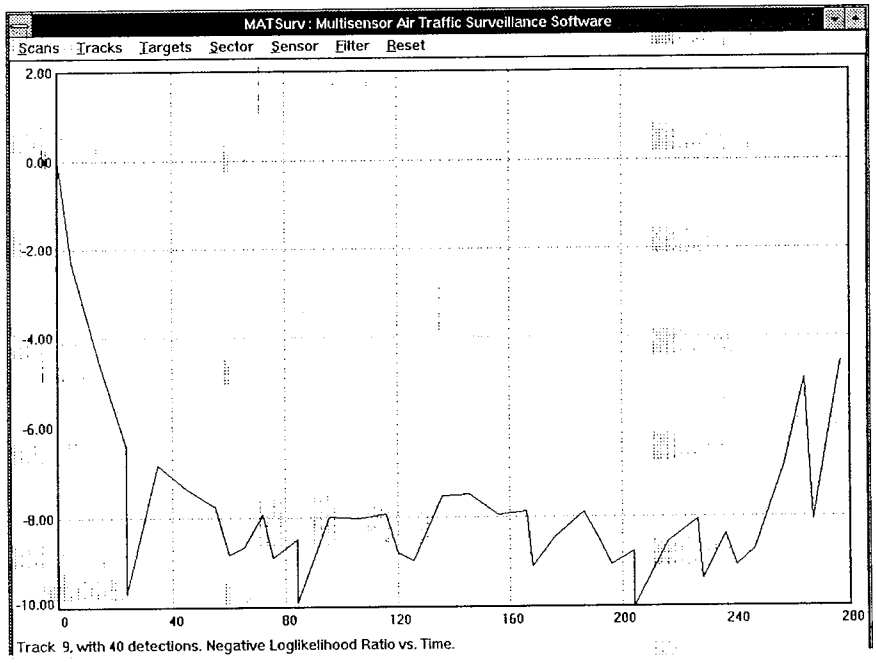

Figure 35: Example 3. Output of tracking filter: Negative log-likelihood ratio, using association

The log-likelihood ratio is consistently below zero, hence all the detections are deemed "true"

7 Discussion

In this section we shall discuss the major results of phase 1 and phase 2 of this project. An interactive software, MATSurv : Multisensor Air Traffic Surveillance, that runs in MS-Windows (version 3.0 or higher) has been developed to analyze the performance of the association algorithm and display the results in a graphical format.

The results of phase 1 relate to the performance of the tracking filter applied to measurements classified using the ID (designated as `iffcode` in the database). These results helped in arriving at the best choice of the design parameters for optimal filter performance. The measurement database (in file `data.bin`) from the two FAA radars contained detections of targets that were in a variety of trajectories. While many of these target trajectories could be described by a straightforward 2^{nd} order motion model with a low process noise, there were some maneuvering targets that would require at least a 2^{nd} order (or 3^{nd} order) motion model with considerable process noise. Since the same tracking filter is required to handle these two extreme cases, the choice of the design paramenters has to be necessarily conservative, i.e., tuned to handle the worst case. This requires trading off some of the achievable estimation accuracy for an enhanced ability to track targets during maneuver.

The above observation clearly indicates that replacing the Kalman filter (the central block in the tracking filter shown in figure 4) with an Interacting Multiple Model filter[2] would make the above design trade-off unnecessary and will enhance the performance.

In phase 2, the measurements were stripped of their IDs and processed using our assignment algorithm. The results obtained indicate that the association algorithm provides a *superior classification* of the measurements into tracks (i.e., trajectories of the hypothesized targets) than compared to the target trajectories obtained using the measurements IDs. The multiplicity of targets assigned to the same ID prevents the exclusive reliance on the target ID, and its use in evaluating the performance of the association algorithm is clearly inappropriate. A particular track formed by the association algorithm has, in general, a few measurements less than the

corresponding target trajectory obtained using the IDs. This is primarily due to the fact that the association algorithm rejects measurements (i.e., *outliers*) that deviate considerably from the established track. Discarding these measurements yields a *better estimate* of the trajectory than the one obtained by including these outlying measurements.

8 Future Work

The following are some of the major issues that are worthy of attention in the future.

- Incorporation of partial 2D measurements (skin returns) into the overall association-estimation framework. These 2D measurements can be used in the enhancing the purity of an established track formed using the full 3D measurements (beacon returns).

- The use of an Interacting Multiple Model estimator to handle both maneuvering and non-maneuvering targets with maximum accuracy.

- Real-time operation.

- The 2-dimensional assignment algorithm used in the present context can be extended to the more general S-dimensional case. The near optimal results obtained using 2D assignment for the currently available measurement database, suggest that in order to fully utilize the advanced features of the S-D assignment, a measurement database that contains a more complex scenario is needed.

- Of more theoretical interest is the issue of modifying the currently used ML formulation of the data association problem to a more general MAP or MMSE kind of a formulation. This would require further modifications to the auction algorithm wherein successive 2D assignments are aggregated into MAP trajectory estimates based on the measurement data.

A Negative-Time Update

In this section we outline the negative time update procedure used in our implementation of the tracking filter. In this case the time interval $\delta_k = t_{k+1} - t_k$ is negative. In the standard case (i.e., $\delta_k > 0$) the past is completely described by the current estimate (i.e., it is the sufficient statistic): $\mathbf{x}_{L_k}(k|k)$ in the local coordinate frame. In the present context (i.e., for negative time update) $\mathbf{x}_{L_k}(k|k)$ is no longer the sufficient statistic, and determination of the optimal – i.e., the minimum mean squared error (MMSE) – estimate requires the knowledge of past data (i.e, $\mathbf{x}_g(k-1|k-1)$, $\mathbf{z}_g(k-1)$ etc.) Since only the updated state and covariance are stored our implementation, the following sub-optimal approach is used for negative time updates.

We "predict" the state at t_{k+1} by propagating the state equation backwards *without process noise* i.e.,

$$\mathbf{x}_{L_k}(k+1|k) = \Phi_k \, \mathbf{x}_{L_k}(k|k) \tag{25}$$

$$P_{L_k}(k+1|k) = \Phi_k \, P_{L_k}(k+1|k) \, \Phi_k' \tag{26}$$

where Φ_k is the (backwards) transition matrix from t_k to t_{k+1}. Since the latest time instant is t_k and not t_{k+1}, the desired updated state should be at t_k (in the standard case it is at t_{k+1}). The state is updated directly using $\mathbf{x}_{L_k}(k+1|k)$ as the "predicted" state, i.e.,

$$\nu_{L_k}(k+1) = \mathbf{z}_{L_k}(k+1) - H \, \mathbf{x}_{L_k}(k+1|k) \tag{27}$$

$$S_{L_k}(k+1) = H \, P_{L_k}(k+1|k) \, H' + R_{L_k}(k+1) \tag{28}$$

$$W_{L_k}(k+1) = P_{L_k}(k+1|k) \, H' \, S_{L_k}(k+1)^{-1} \tag{29}$$

$$\mathbf{x}^{\star}_{L_k}(k|k) = \mathbf{x}_{L_k}(k|k) + W_{L_k}(k+1) \, \nu_{L_k}(k+1) \tag{30}$$

$$P^{\star}_{L_k}(k|k) = P_{L_k}(k|k) - W_{L_k}(k+1) \, S_{L_k}(k+1) \, W_{L_k}(k+1)' \tag{31}$$

The state estimate $\mathbf{x}_{L_k}(k|k)$ and covariance $P_{L_k}(k|k)$) are now updated to $\mathbf{x}^{\star}_{L_k}(k|k)$ and $P^{\star}_{L_k}(k|k)$ respectively. This method has been found to be quite satisfactory in all the instances where negative time updates were required.

References

[1] Deb, S., Pattipati, K. R., Bar-Shalom, Y. and Washburn, R., "A new relaxation algorithm and passive sensor data association", *IEEE Transactions on Automatic Control*, Vol. AC-37, No. 2, Feb. 1992.

[2] Bar-Shalom, Y. and Li, X. R. *Estimation and Tracking: Principles, Techniques and Software.* Norwood, MA: Artech House 1993.

[3] Hilton, R. D, Martin, D. A., and Blair, W. D, "Tracking with time-delayed data in multisensor systems", Tech. Rep. NSWCDD/TR-93/351, Naval Surface Warfare Center, Dahlgren Division, Aug. 1993.

*U.S. GOVERNMENT PRINTING OFFICE: 1995-610-126-50139

MISSION

OF

ROME LABORATORY

Mission. The mission of Rome Laboratory is to advance the science and technologies of command, control, communications and intelligence and to transition them into systems to meet customer needs. To achieve this, Rome Lab:

a. Conducts vigorous research, development and test programs in all applicable technologies;

b. Transitions technology to current and future systems to improve operational capability, readiness, and supportability;

c. Provides a full range of technical support to Air Force Materiel Command product centers and other Air Force organizations;

d. Promotes transfer of technology to the private sector;

e. Maintains leading edge technological expertise in the areas of surveillance, communications, command and control, intelligence, reliability science, electro-magnetic technology, photonics, signal processing, and computational science.

The thrust areas of technical competence include: Surveillance, Communications, Command and Control, Intelligence, Signal Processing, Computer Science and Technology, Electromagnetic Technology, Photonics and Reliability Sciences.